

## References and Notes

- R. Revelle and H. Suess, *Tellus* **9**, 18 (1959); B. Bolin and E. Ericksson, in *The Atmosphere and the Sea in Motion*, Rossby Memorial Volume, B. Bolin, Ed. (Rockefeller Institute Press, New York, 1959), p. 130; W. S. Broecker, T. Takahashi, H. J. Simpson, T.-H. Peng, *Science* **206**, 409 (1979).
- R. M. Rotty, in *The Fate of Fossil Fuel CO<sub>2</sub> in the Oceans*, N. Andersen and A. Malahoff, Eds. (Plenum, New York, 1977), p. 167; R. Rotty and G. Marland [Document ORAM-IEA-80-9(M), Institute for Energy Analysis, Oak Ridge Associated Universities, Oak Ridge, Tenn., 1980].
- J. Hansen *et al.*, *Science* **213**, 957 (1981); M. C. MacCracken, *ibid.* **220**, 873 (1983); J. Hansen *et al.*, *ibid.*, p. 874.
- T. Takahashi, W. S. Broecker, A. E. Bainbridge, R. F. Weiss, "Carbonate chemistry of the Atlantic, Pacific, and Indian oceans: Results of the GEOSECS Expedition 1972-1978" (Technical Report No. ICU-1-8, Lamont-Doherty Geological Observatory, Palisades, N.Y., 1980).
- C. Culberson and R. M. Pytkowicz, *Limnol. Oceanogr.* **13**, 403 (1968).
- C. Mehrbach, C. Culberson, J. E. Hawley, R. M. Pytkowicz, *ibid.* **18**, 897 (1973).
- F. J. Millero, *Geochim. Cosmochim. Acta* **43**, 1651 (1979).
- S. Honjo, *J. Mar. Res.* **38**, 53 (1980).
- R. C. Thunell and S. Honjo, *Mar. Geol.* **40**, 237 (1981).
- S. Tsunogai, M. Uematsu, S. Noriki, N. Tanaka, M. Yamada, *Geochim. J.* **16**, 129 (1982).
- R. A. Feely and C. T. A. Chen, *Geophys. Res. Lett.* **9**, 1294 (1982); R. A. Feely, R. H. Byrne, P. R. Betzer, J. F. Gendron, J. G. Acker, *J. Geophys. Res.*, in press.
- M. Fiadeiro, *Earth Planet. Sci. Lett.* **49**, 499 (1980).
- R. H. Byrne, J. G. Acker, P. R. Betzer, R. A. Feely, M. Cates, *Nature (London)*, in press.
- A. Soutar, S. A. Kline, E. Duffrin, K. W. Bruland, *Nature (London)* **266**, 136 (1977).
- P. R. Betzer *et al.*, *Deep Sea Res.* **31**, 1 (1984).
- J. W. Morse, A. Mucci, F. W. Millero, *Geochim. Cosmochim. Acta* **44**, 85 (1980).
- A. W. H. Bé and R. W. Gilmer, *Oceanic Micropaleontology*, A. T. S. Ramsay, Ed. (Academic Press, New York, 1977), p. 733.
- J. A. McGowan, in *The Micropaleontology of Oceans*, B. M. Funnell and W. R. Riedel, Eds. (Cambridge Univ. Press, Cambridge, 1971), p. 3; in *The Biology of the Oceanic Pacific*, C. B. Miller, Ed. (Proceedings of the 33rd Annual Biology Colloquium) (Oregon State Univ. Press, Corvallis, 1974), p. 9; J. L. Reid, E. Brinton, A. Fleminger, E. L. Venrick, J. A. McGowan, in *Advances in Oceanography*, H. Charnock and G. Deacon, Eds. (Plenum, New York, 1978), p. 65.
- W. H. Berger, C. G. Adelseck, L. A. Mayer, *J. Geophys. Res.* **81**, 2617 (1976).
- R. A. Berner, *The Fate of Fossil Fuel CO<sub>2</sub> in the Oceans*, N. Andersen and A. Malahoff, Eds. (Plenum, New York, 1977), p. 243.
- S. Honjo, *ibid.*, p. 269.
- R. A. Berner, *Ambio Special Rep. No. 6* (1979), p. 5.
- \_\_\_\_\_ and S. Honjo, *Science* **211**, 940 (1981).
- P. R. Betzer, R. H. Byrne, R. A. Feely, *Eos* **63** (No. 3), 45 (1982) (abstract).
- W. D. Gardner, K. R. Hinga, J. Marra, *J. Mar. Res.* **41**, 195 (1983).
- J. K. Bishop, J. M. Edmond, D. R. Ketten, M. P. Bacon, W. B. Silker, *Deep Sea Res.* **24**, 511 (1977); D. A. Fellows, D. M. Karl, G. A. Knauer, *ibid.* **28**, 921 (1981).
- S. Tsunogai and Y. Watanabe, *Geochem. J.* **15**, 95 (1981).
- I. N. Plummer and E. T. Sundquist, *Geochim. Cosmochim. Acta* **46**, 247 (1982).
- A. C. Hardy, in *The Open Sea. Its Natural History: The World of Plankton* (Collins, London, 1956); I. A. MacLaren, *J. Fish. Res. Board Can.* **20** (No. 3), 685 (1963); M. F. Vinogradov, in *The Vertical Distribution of the Oceanic Zooplankton* (Publication TT-69-59015, National Technical Information Service, Springfield, Va., 1970).
- We thank Captain R. Speer and the crew of the R.V. *Discoverer*, who were especially effective throughout the cruise. We owe a special tribute to Chief Bosun W. Sherril and the deck crew whose hard and competent work made possible multiple launchings and retrievals of the free-drifting sediment traps. We thank J. Cline who was always prepared to solve problems and D. Jones and A. King who provided logistical help prior to the cruise. We express special thanks to J. A. McGowan for encouragement and help with this project. This research was supported by a grant from the Air Resources Laboratory under the direction of L. Machta to the University of South Florida (NA80RAD00020). Contribution No. 735 from Pacific Marine Environmental Laboratory.

29 June 1984; accepted 14 September 1984

ruption of the *c-myb* locus and transcription of an altered form of *c-myb* in ABPL's could result in the induction, progression, or maintenance of these tumors.

In elucidating the mechanism by which the *c-myb* locus is rearranged in the ABPL's, the *c-myb* locus of four ABPL's was first examined at the DNA level. Normal BALB/c liver and ABPL DNA's were digested with Eco RI and analyzed by the method of Southern (4) (Fig. 1). The DNA's were first probed (Fig. 1A) with the avian *v-myb* sequence isolated as a 1.3-kilobase-pair (kbp) Kpn I-Xba I fragment from a chicken AMV proviral clone (5, 6). In addition to the 4.2-, 2.0-, 1.7-, and 1.5-kbp *myb* hybridizing bands in normal BALB/c liver DNA, each of the four ABPL's contained a larger band of varying size. In experiments to determine which part of the *c-myb* locus was altered, a 0.5-kbp Kpn I-Eco RI fragment which represents the 5' half of the *v-myb* was isolated from a chicken AMV provirus clone ( $\lambda$ 11A-1-1) (6). When this was used as a probe, only the 4.2-kbp band and the rearranged *myb* bands showed hybridization (Fig. 1B). This indicates that the 4.2-kbp Eco RI fragment contained the portion of *c-myb* homologous with the 5' *v-myb* region and that this fragment was altered in the ABPL's, giving rise to the larger Eco RI fragments. Furthermore, when the DNA's were probed with a 0.8-kbp Eco RI-Xba I fragment which represents the 3' half of the *v-myb* sequence, only the smaller bands but not the 4.2-kbp or the rearranged Eco RI fragments showed hybridization (data not shown). Hence, the rearrangement had occurred at the 5' end of the *c-myb* locus in each of these four ABPL's. Presumably, it is this rearrangement in the *c-myb* locus in ABPL's that results in the synthesis of the larger *myb* RNA transcripts that have been described (1).

To study the altered *myb* locus in ABPL's, we cloned these sequences from Eco RI-digested genomic DNA's from four of the ABPL's with the use of  $\lambda$ gt WES  $\cdot$   $\lambda$ B vectors (7). The recombinant  $\lambda$  clones were selected by hybridization with *v-myb*. Unrearranged *c-myb* sequences were also obtained by screening a bacteriophage library of BALB/c mouse DNA (partial Eco RI\* digest). The Eco RI insert from each of these clones was subcloned in pBR322 and used in all subsequent studies.

For elucidation of the molecular nature of the DNA rearrangement, the 7.5-kbp Eco RI insert from ABPL2 was hybridized to the corresponding 4.2-kbp Eco RI fragment of the normal *c-myb*

## Activation of the *c-myb* Locus by Viral Insertional Mutagenesis in Plasmacytoid Lymphosarcomas

**Abstract.** *Rearrangement in the c-myb locus of each of four independently derived BALB/c plasmacytoid lymphosarcoma (ABPL's) is due to the insertion of a defective Moloney murine leukemia virus (M-MuLV) into a 1.5-kilobase-pair stretch of cellular DNA at the 5' end of the v-myb-related sequences. This retroviral insertion is associated with abnormal transcription of myb sequences and probably represents a step in the neoplastic transformation of ABPL cells.*

Three types of B lymphocytic tumors arise in BALB/c mice after they receive intraperitoneal injections of pristane and Abelson virus. On the basis of their morphology and association with Abelson virus these tumors are termed lymphosarcomas (ABLS's), plasmacytomas (ABPC's), and plasmacytoid lymphosarcomas (ABPL's) (1). The Abelson virus used in the tumor induction contained two retroviral elements: the replication-defective, transforming Abelson murine leukemia virus (A-MuLV) and the transmissible helper Moloney murine leukemia virus (M-MuLV). Both viral elements have the same 5' and 3' ends of the viral genome, including two long

terminal repeats (LTR's). The central portion of the M-MuLV gene has been replaced by the transforming *v-abl* sequence in A-MuLV (2). All ABLS's and ABPC's contain integrated A-MuLV proviral genomes and synthesize abundant *v-abl* RNA, while ABPL's do not (1). Instead, each of the ABPL's has undergone a DNA rearrangement in one of the *c-myb* loci, resulting in the synthesis of abnormal messenger RNA transcripts (1). Because *c-myb* is the cellular homolog of viral *myb* (*v-myb*) of avian myeloblastosis virus (AMV) and because the *v-myb* sequence is thought to be essential for the oncogenic properties of AMV in certain target cells (3), the dis-

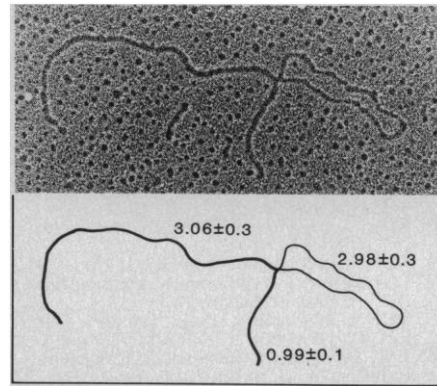
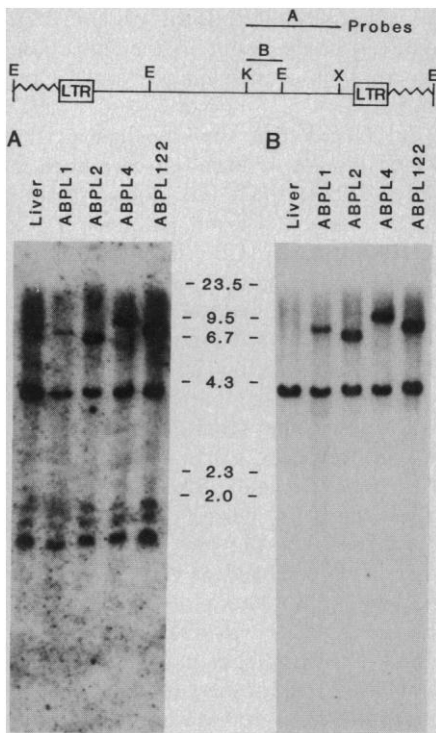


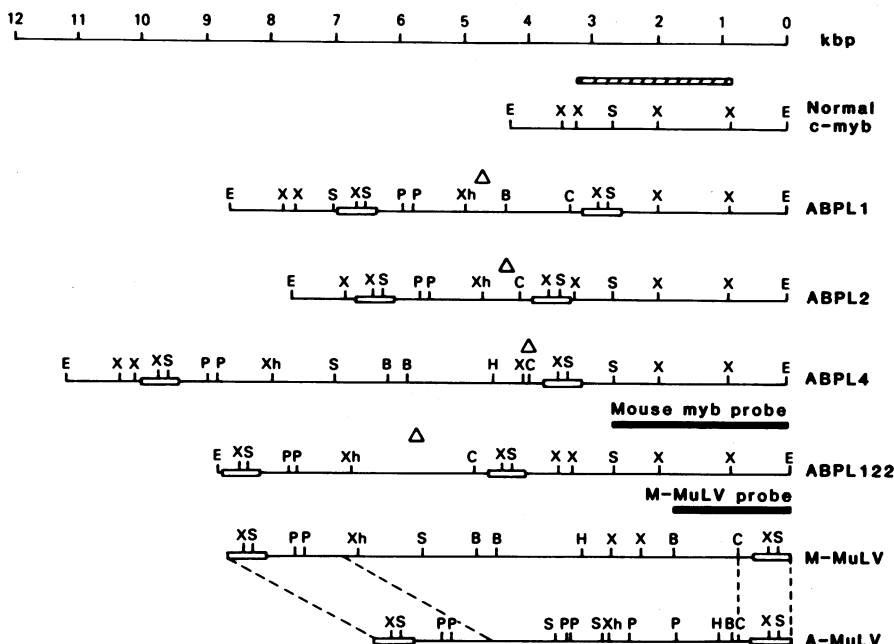
Fig. 1 (left). *Myb* hybridization of blots of Eco RI digests of genomic DNA (15  $\mu$ g) from BALB/c liver and ABPL's as indicated. The conditions for preparation of Southern blot filters, low stringency hybridization, and washings were as described (1). The diagram above the blots shows the restriction map of the AMV provirus clone ( $\lambda$  11A-1-1) (6) containing the *myb* probes used for (A) and (B). The probe used for (A) was a 1.3-kbp Kpn I-Xba I fragment, and that used for (B) was a 0.5-kbp Kpn I-Eco RI fragment containing the 5' portion of *v-myb*. The sizes of standard markers (Hind III fragments of phage  $\lambda$  DNA) in (A) and of the hybridization bands in

(B) are in kilobase pairs. E, Eco RI; K, Kpn I; X, Xba I. Fig. 2 (right). Electron micrograph of a heteroduplex formed between the 4.2-kbp Eco RI fragment of normal mouse *c-myb* DNA and the 7.5-kbp Eco RI fragment of ABPL2 DNA. A diagrammatic representation of the heteroduplex is shown below the electron micrograph. Contour lengths are in kilobase pairs.

DNA, and the resultant heteroduplexes were examined under an electron microscope. The results (Fig. 2) indicated that the two DNA fragments shared homology of 0.99 kbp and 3.0 kbp at the two ends and that the rearranged *myb* fragment from ABPL2 tumor contained a large insertion of approximately 3.0 kbp toward one end of the fragment.

To determine whether the insertion

could be due to the remnants of the viral components used in the induction of the ABPL's, we examined the four ABPL *myb* clones for the retroviral LTR sequences. Southern blot analysis (not shown) demonstrated that each of the rearranged *myb* clones contained two MuLV-LTR sequences. This was also confirmed by comparative restriction map analysis of the normal *c-myb* DNA



and of its rearranged counterparts in ABPL's (Fig. 3). Analysis of the restriction maps revealed the similarity of restriction sites such as Pst I, Xho I, and Cla I in the sequences between the LTR's, suggesting that a common viral element had inserted into the *c-myb* locus. However, the restriction sites between the LTR's in ABPL *myb* clones did not correlate with those of A-MuLV sequence. Instead, the pattern was strikingly similar to M-MuLV, the helper virus in the preparation used to induce ABPL's. Thus it appears that, in each of the four tumors, a M-MuLV had integrated in a 5' to 3' orientation within a 1.5-kbp region upstream from the sequences homologous with the 5' portion of the *v-myb* sequence. The position of sequences homologous with *v-myb* and the LTR's in each clone were determined, respectively, by *v-myb* and M-MuLV-LTR hybridization of blots with appropriate restriction digests of the four recombinant clones. Each rearranged clone can be divided into two major unequal fragments by digesting with Eco RI and Pst I. In each case, the larger restriction fragment hybridized to the *v-myb* probe, while both fragments hybridized to the M-MuLV-LTR-specific probe (data not shown).

To verify further and to locate the integration of the M-MuLV proviral genome in the ABPL *myb* locus, we analyzed heteroduplexes formed between a M-MuLV proviral insert and each of the ABPL rearranged *myb* clones. One such result, for the ABPL1 *myb* clone, is shown in Fig. 4. The single loop in the heteroduplex indicated a deletion in the middle region of the M-MuLV, while the rest of the ABPL proviral sequences appeared to be completely homologous with the M-MuLV

Fig. 3. Restriction maps of the four cloned rearranged *myb* genes from ABPL1, ABPL2, ABPL4, and ABPL122. The region (striped box) containing sequences homologous with the 5' portion of the *v-myb* gene was determined by heteroduplex analysis (data not shown) and *v-myb* hybridization of blots with appropriate restriction digests of the four recombinant clones. The positions of retroviral LTR's (open rectangular boxes) were determined by M-MuLV-LTR hybridization of blots of the clones. The restriction maps of M-MuLV (16) and A-MuLV (17) are included in this figure for comparison. Dashed lines indicate portions that are identical between the two viruses on the basis of results from nucleotide sequence analysis (18). The region in which an internal deletion had occurred within the M-MuLV inserts in ABPL clones ( $\Delta$ ) was determined by restriction mapping and heteroduplex analysis. Abbreviations: E, Eco RI; B, Bam HI; H, Hind III; Xh, Xho I; S, Sac I; C, Cla I; P, Pst I; and X, Xba I.

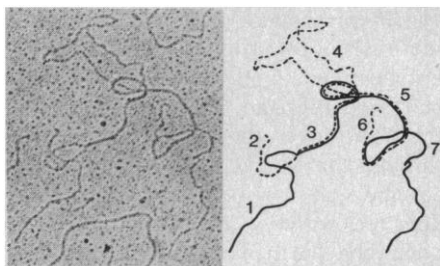


Fig. 4. Heteroduplex analysis of the M-MuLV-Eco RI proviral insert isolated from infected rat cells with the cloned Eco RI rearranged *myb* fragments from ABPL1. The 10.9-kbp Eco RI fragment of M-MuLV proviral insert and the plasmid subclones of the 8.7-kbp Eco RI fragment of ABPL1 were digested with Eco RI, denatured, reannealed under stringent conditions, and spread for electron microscopy as described (19). Regions of the heteroduplexes are indicated on the tracings as follows. 1, ABPL cellular sequence; 2, 1.4-kb rat cellular sequence flanking the M-MuLV 5' LTR; 3, duplex region of ABPL sequence hybridized with the 5' portion of M-MuLV sequence; 4, deletion loop of M-MuLV sequence; 5, duplex region of ABPL sequence with the 3' portion of M-MuLV sequence; 6, 0.7-kb rat cellular sequence flanking the M-MuLV 3' LTR; 7, ABPL cellular sequence containing sequences homologous with the *v-myb* gene.

with no evidence of substitution loops. The different ABPL clones showed similar heteroduplex patterns, differing only in the lengths of the single-stranded loop. The variations in the length of the rearranged *myb*-Eco RI fragments in the ABPL's were due to varying extents of internal deletions in the *gag*, *pol*, or *env* regions. However, each proviral genome retained both LTR's and adjacent sequences essential for viral DNA synthesis, integration, transcription, and packaging (8).

Further characterization of the inserted M-MuLV proviral genome in the *c-myb* locus was carried out by nucleotide sequence analysis of a pBR322 subclone containing the 7.5-kbp Eco RI insert of ABPL2. Cleavage by *Sac* I occurred within each of the M-MuLV LTR's, yielding a 3.0-kbp proviral fragment. This fragment was sequenced in its entirety and was found to be homologous with the sequence of M-MuLV (9) at the 5' end up to position 2040 and from position 7521 to the 3' end of the genome. This confirms the results of restriction and heteroduplex analyses showing that the inserted DNA contains a partial M-MuLV genome that has had deletions in *gag*, *pol*, and *env* genes. In the sequences of ABPL2 surrounding the deletion (Fig. 5), there was a direct repeat of seven bases, AGAGAGA (A, adenine; G, guanine), at the precise point

of deletion and an inverted repeat of seven bases, TTGGCCA (T, thymidine; C, cytosine), in the deleted portion of the M-MuLV sequences a few bases from the direct repeat sequences. These repeated sequences might play a role in the deletion of the *gag*, *pol*, and *env* sequences in the M-MuLV proviral genome.

Earlier we showed that *c-myb* expression in ABPL's is altered (1). Particularly large elevations in the amount of *myb* RNA were found in ABPL1, ABPL2, and ABPL122. In addition, the tumors also contained *myb* RNA's larger than the 3.8- and 4.2-kb *myb* RNA's present in the thymus. The size of these ABPL-specific *myb* RNA's varied among the tumors but was usually around 5.0 kb.

Apparently the insertion of the M-MuLV increased both the size and amount of the *c-myb* transcripts. The insertion of a defective M-MuLV proviral genome in a 5' to 3' orientation upstream from the *v-myb*-related sequences in ABPL's appears to be analogous to the insertion of avian leukosis virus (ALV) in the *c-myc* locus of most bursal lymphomas (10). However, when blots of the ABPL RNA's were hybridized with a probe that contains the M-MuLV-LTR sequence, only the 8.8-kb M-MuLV genomic RNA and the 3.3-kb subgenomic RNA species were detected (data not shown). Additional hybridization studies with other parts of the M-MuLV genome have indicated that the abnormal ABPL *myb* RNA's do not appear to contain any M-MuLV sequence. Hence, unlike the abnormal *myc* RNA's in most avian lymphomas, the M-MuLV proviral inserts probably increase *myb* transcription not by promoter insertion but rather by an enhancing mechanism or by dissociating the *myb* coding regions from upstream regulatory sequences. The disruption within the *myb* gene may also have been responsible for the unusually large sizes of the ABPL *myb* RNA species, which probably represented abnormally spliced transcripts. These altered messengers may have open reading frames different from the normal *myb* transcript and may encode abnormal *myb* proteins. The *myb* transcripts do not contain RNA from the inserted M-MuLV proviral DNA. Whether the proviral inserts were not transcribed or were spliced out requires more detailed analysis. Understanding the altered *myb* transcription in ABPL's could provide some insight into the role of *myb* in tumorigenesis in view of the recent findings that sequences related to *c-myb* were expressed in nine of ten

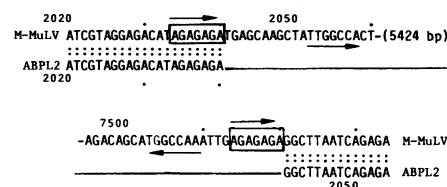


Fig. 5. Location of the deletion point in the M-MuLV insert in ABPL2 DNA. The top line gives the published sequence of M-MuLV (9), and the bottom line gives the sequence of the ABPL2 DNA in the region where the deletion is observed. The 7-base direct repeat in the M-MuLV genome present at the point of deletion is boxed. The inverted repeats are indicated by arrows.

human hematologic malignancies examined (11).

Tumors of hematopoietic cells are believed to represent frozen stages of differentiation. The transcription of *c-myb* gene is found in precursor cells of the lymphoid, myeloid, and erythroid series but not in more differentiated cells, indicating that *c-myb* expression appears to be restricted to immature hematopoietic cells (12). The constitutive expression of the altered *c-myb* locus as a result of M-MuLV proviral integration in ABPL's may be closely linked to the proliferation of these immature hematopoietic cells. Although these data do not provide direct evidence that the observed proviral insertions acted in ABPL tumorigenesis, it is highly unlikely that random integration events would result in four of four tumors having a provirus inserted within a 1.5-kbp region in the *c-myb* locus. In addition, *myb* rearrangement was found in two other ABPL's on the basis of results from Southern blot analysis (1, 4). The tumor-specific *myb* fragments in these two tumors contained restriction sites characteristic of a M-MuLV provirus (data not shown). This provides strong evidence that M-MuLV can induce tumors by insertional mutagenesis. The mechanism of tumorigenesis of other tumors such as ALV-induced lymphomas (10) and mouse mammary tumor virus-induced carcinomas (13) is also thought to be insertional mutagenesis.

Earlier we proposed that the ABPL's resulted from a "hit and run" mechanism whereby an A-MuLV proviral genome is initially integrated but subsequently excised. These results suggest that insertion of M-MuLV rather than A-MuLV in a specific integration site in the *myb* locus is a critical event in ABPL tumorigenesis. The role of the A-MuLV (if it has one) is not currently known. Even though A-MuLV has the same LTR's as M-MuLV, it has not been found to insert in the *myb* locus in the

tumors examined. It is possible that A-MuLV could have initiated an early step in ABPL tumorigenesis but it was not required for the maintenance of the neoplastic state, as was shown for several pre-B lymphosarcomas (14). Elimination of A-MuLV genome may have favored survival of that cell type because the gene product of *v-abl* has been shown to be toxic to certain cell types (15). Whether ABPL's can be induced by M-MuLV alone or by a concerted effort between the two viral elements in Abelson virus remains to be tested.

GRACE L. C. SHEN-ONG  
MICHAEL POTTER  
J. FREDERIC MUSHINSKI

Laboratory of Genetics,  
National Cancer Institute,  
Bethesda, Maryland 20205

SUKADEV LAVU  
E. PREMKUMAR REDDY  
Laboratory of Cellular and Molecular  
Biology, National Cancer Institute

#### References and Notes

1. J. F. Mushinski, M. Potter, S. R. Bauer, E. P. Reddy, *Science* **220**, 795 (1983).
2. A. Shields, S. Goff, M. Paskind, G. Otto, D. Baltimore, *Cell* **18**, 955 (1979); S. P. Goff, E. Gilboa, O. N. Witte, D. Baltimore, *ibid.* **22**, 777 (1980).

3. P. H. Duesberg, K. Bister, C. Moscovici, *Proc. Natl. Acad. Sci. U.S.A.* **77**, 5120 (1980); L. M. Souza, J. N. Strommer, R. L. Hilyard, M. C. Komaromy, M. A. Baluda, *ibid.*, p. 5177; T. J. Gonda *et al.*, *Cell* **23**, 279 (1981).
4. E. Southern, *J. Mol. Biol.* **98**, 503 (1975).
5. L. M. Souza, M. J. Briskin, R. L. Hilyard, M. A. Baluda, *J. Virol.* **36**, 325 (1980).
6. K. E. Rushlow *et al.*, *Science* **216**, 1421 (1982).
7. P. Leder, D. Tiemeier, L. Enquist, *ibid.* **196**, 175 (1977).
8. H. E. Varmus, *ibid.* **216**, 812 (1982).
9. T. M. Shinnick, R. A. Lerner, J. G. Sutcliffe, *Nature (London)* **293**, 543 (1981).
10. W. S. Hayward, B. G. Neel, S. M. Astrin, *ibid.* **290**, 475 (1981); B. G. Neel, W. S. Hayward, H. Robinson, J. Fang, S. M. Astrin, *Cell* **23**, 323 (1981); G. S. Payne, J. M. Bishop, H. E. Varmus, *Nature (London)* **295**, 209 (1982).
11. D. J. Slamon, J. B. deKernion, I. M. Verma, M. J. Cline, *Science* **224**, 256 (1984).
12. E. H. Westin *et al.*, *Proc. Natl. Acad. Sci. U.S.A.* **79**, 2194 (1982).
13. R. Nusse and H. E. Varmus, *Cell* **31**, 99 (1982); G. Peters, S. Brooks, R. Smith, C. Dickson, *ibid.* **33**, 369 (1983).
14. D. J. Grunwald *et al.*, *J. Virol.* **43**, 92 (1982).
15. S. F. Ziegler, C. A. Whitlock, S. P. Goff, A. Gifford, O. N. Witte, *Cell* **27**, 477 (1981).
16. A. Srinivasan, E. P. Reddy, S. A. Aaronson, *Proc. Natl. Acad. Sci. U.S.A.* **78**, 2077 (1981).
17. S. A. Latt, S. P. Goff, C. J. Tabin, M. Paskind, J.Y.-J. Wang, D. Baltimore *J. Virol.* **45**, 1195 (1983).
18. E. P. Reddy, M. J. Smith, A. Srinivasan, *Proc. Natl. Acad. Sci. U.S.A.* **80**, 3623 and 7372 (1983).
19. R. W. Davis, M. Simon, N. Davidson, *Methods Enzymol.* **21**, 413 (1971).
20. We thank S. Tronick for the generous use of electron microscopy facilities, B. K. Birshstein and L. A. Eckhart for the bacteriophage library of BALB/c mouse DNA, and M. Millison and V. Rogers for editorial assistance.

11 June 1984; accepted 21 August 1984

## Expression of the *c-fos* Gene and of a *fos*-Related Gene Is Stimulated by Platelet-Derived Growth Factor

**Abstract.** Complementary DNA clones of genes induced by platelet-derived growth factor (PDGF) in BALB/c-3T3 cells were isolated; one such clone contains a domain having nucleotide sequence homology with the third exon of *c-fos*. This nucleotide sequence homology is reflected in the predicted amino acid sequences of the gene products. Under low stringency conditions, the mouse *v-fos* gene cross-hybridizes with the PDGF-inducible complementary DNA clone. However, the messenger RNA transcripts of mouse *c-fos* and the new *fos*-related gene can be distinguished by gel electrophoresis and by S1 nuclease analysis. Expression of the authentic *c-fos* gene is induced by PDGF and superinduced by the combination of PDGF and cycloheximide.

We have described the isolation of a platelet-derived growth factor (PDGF)-inducible complementary DNA (cDNA) clone termed "pBC-JB" (1). Subfragments of pBC-JB were cloned into M13 mp8 and sequenced by the dideoxy method (2). The nucleotide sequence thus derived was screened for relationships to other genes recorded in the Genbank data base with a rapid similarity search algorithm of Wilbur and Lipman (3). This screen indicated that the pBC-JB cDNA insert (hereafter abbreviated as "*r-fos*") contained a domain with nucleotide sequence homology to the third exon of the mouse *c-fos* gene (4). The nucleotide sequence of this homolo-

gous region and the flanking sequences of *r-fos* which show little or no homology to the second and fourth exons of *c-fos*, are shown in Fig. 1.

The third exon of mouse *c-fos* contains an open reading frame encoding 36 amino acids. This sequence of 36 amino acids is strongly conserved between mouse *c-fos*, its viral homolog, and human *c-fos* (5). The domain of *r-fos*, which is homologous to the *c-fos* third exon, is contained within the longest open reading frame of the cDNA clone. This reading frame dictates synthesis of a peptide similar to that directed by the corresponding region of *c-fos* messenger RNA (mRNA) (Fig. 1). The *r-fos* cDNA

clone represents only about 50 percent of the mRNA. We cannot detect an ATG (A, adenine; T, thymine; G, guanine) start signal for the longest open reading frame; however, this frame is contiguous through the 5' end of the clone. If we assume that the longest reading frame depicted within *r-fos* is the authentic one, then the nucleotide sequence homology between *r-fos* and *c-fos* is reflected at the amino acid level.

The sequence homology between *r-fos* and *c-fos* is pervasive enough to suggest that these two genes would cross-hybridize with each other under relaxed stringency conditions. Southern gel electrophoresis (Fig. 2) (6) confirms this prediction.

Although there is sufficient sequence homology to allow cross hybridization of *r-fos* and *c-fos* DNA's at relaxed stringency, the mRNA's corresponding to these two genes can be readily distinguished by gel electrophoresis (Fig. 3). By sequentially probing a Northern blot (7) filter with nick-translated *v-fos* and then with *r-fos*, we were able to demonstrate differences in the molecular weight of their cognate mRNA's. A single band of mRNA that reacted with the *v-fos* probe (8) migrated with an apparent molecular weight of 2.2 kb (5). Another band reacting with the *r-fos* probe has an apparent molecular weight of about 2.0 kb. The *r-fos* mRNA appears to be more abundant than *c-fos* in these Northern blots (Fig. 3).

The Northern gel assay shown in Fig. 3 required isolation of poly(A)<sup>+</sup> (polyadenylated) RNA from large quantities of cell cultures. For this reason we were forced to use partially purified PDGF preparations in the experiment. To establish that PDGF itself, rather than some other agent within platelet extracts, regulates *c-fos* expression, we developed a *c-fos* probe suitable for S1 nuclease analysis of total cellular RNA in solution. With mouse *v-fos* provirus as a source of starting material, a Pst I restriction fragment homologous to authentic *c-fos* mRNA within a region spanned by the second and third *c-fos* exons was cloned into M13 mp8 bacteriophage. The region spanned by this M13 probe is indicated by the bracketed arrows in Fig. 4. The nucleotide sequence of the M13 probe dictates that *c-fos* mRNA will protect a 234-nucleotide fragment from S1 nuclease digestion. Under identical conditions, *r-fos* mRNA could protect no fragment of the probe greater than 24 nucleotides in length as indicated by the sequence data (Fig. 1). S1 nuclease analysis indicates that